JCI The Journal of Clinical Investigation

In vivo selection of hematopoietic progenitor cells and temozolomide dose intensification in rhesus macaques through lentiviral transduction with a drug resistance gene

Andre Larochelle, … , Cynthia E. Dunbar, Brian P. Sorrentino

J Clin Invest. 2009;119(7):1952-1963. https://doi.org/10.1172/JCI37506.

Research Article

Major limitations to gene therapy using HSCs are low gene transfer efficiency and the inability of most therapeutic genes to confer a selective advantage on the gene-corrected cells. One approach to enrich for gene-modified cells in vivo is to include in the retroviral vector a drug resistance gene, such as the P140K mutant of the DNA repair enzyme O^6-methylguanine-DNA methyltransferase (MGMT*). We transplanted 5 rhesus macaques with $CD34^+$ cells transduced with lentiviral vectors encoding MGMT* and a fluorescent marker, with or without homeobox B4 (*HOXB4*), a potent stem cell self-renewal gene. Transgene expression and common integration sites in lymphoid and myeloid lineages several months after transplantation confirmed transduction of long-term repopulating HSCs. However, all animals showed only a transient increase in gene-marked lymphoid and myeloid cells after O^6-benzylguanine (BG) and temozolomide (TMZ) administration. In 1 animal, cells transduced with MGMT* lentiviral vectors were protected and expanded after multiple courses of BG/TMZ, providing a substantial increase in the maximum tolerated dose of TMZ. Additional cycles of chemotherapy using 1,3-bis-(2-chloroethyl)-1-nitrosourea (BCNU) resulted in similar increases in gene marking levels, but caused high levels of nonhematopoietic toxicity. Inclusion of HOXB4 in the MGMT* vectors resulted in no substantial increase in gene marking or HSC amplification after chemotherapy treatment. Our data therefore suggest that lentivirally mediated gene transfer in transplanted HSCs can provide in […]

In vivo selection of hematopoietic progenitor cells and temozolomide dose intensification in rhesus macaques through lentiviral transduction with a drug resistance gene

Andre Larochelle,[1] Uimook Choi,[2] Yan Shou,[3] Nora Naumann,[2] Natalia A. Loktionova,[4] Joshua R. Clevenger,[1] Allen Krouse,[1] Mark Metzger,[1] Robert E. Donahue,[1] Elizabeth Kang,[2] Clinton Stewart,[5] Derek Persons,[3] Harry L. Malech,[2] Cynthia E. Dunbar,[1] and Brian P. Sorrentino[3]

[1]National Heart, Lung and Blood Institute (NHLBI) and [2]National Institute of Allergy and Infectious Diseases (NIAID), NIH, Bethesda, Maryland, USA. [3]Division of Experimental Hematology, Department of Hematology, St. Jude Children's Research Hospital, Memphis, Tennessee, USA. [4]Department of Cellular and Molecular Physiology, Pennsylvania State University College of Medicine, M.S. Hershey Medical Center, Hershey, Pennsylvania, USA. [5]Department of Pharmaceutical Sciences, St. Jude Children's Research Hospital, Memphis, Tennessee, USA.

Major limitations to gene therapy using HSCs are low gene transfer efficiency and the inability of most therapeutic genes to confer a selective advantage on the gene-corrected cells. One approach to enrich for gene-modified cells in vivo is to include in the retroviral vector a drug resistance gene, such as the P140K mutant of the DNA repair enzyme O^6-methylguanine-DNA methyltransferase (MGMT*). We transplanted 5 rhesus macaques with $CD34^+$ cells transduced with lentiviral vectors encoding MGMT* and a fluorescent marker, with or without homeobox B4 (*HOXB4*), a potent stem cell self-renewal gene. Transgene expression and common integration sites in lymphoid and myeloid lineages several months after transplantation confirmed transduction of long-term repopulating HSCs. However, all animals showed only a transient increase in gene-marked lymphoid and myeloid cells after O^6-benzylguanine (BG) and temozolomide (TMZ) administration. In 1 animal, cells transduced with MGMT* lentiviral vectors were protected and expanded after multiple courses of BG/TMZ, providing a substantial increase in the maximum tolerated dose of TMZ. Additional cycles of chemotherapy using 1,3-bis-(2-chloroethyl)-1-nitrosourea (BCNU) resulted in similar increases in gene marking levels, but caused high levels of nonhematopoietic toxicity. Inclusion of HOXB4 in the MGMT* vectors resulted in no substantial increase in gene marking or HSC amplification after chemotherapy treatment. Our data therefore suggest that lentivirally mediated gene transfer in transplanted HSCs can provide in vivo chemoprotection of progenitor cells, although selection of long-term repopulating HSCs was not seen.

Introduction

Retroviral vector–mediated gene transfer into HSCs has the potential to improve treatment for various genetic, malignant, and infectious diseases (1, 2). However, a critical limitation to stem cell gene therapy is the low gene transfer efficiency in large animal models and clinical trials (3, 4).

In a recent gene therapy trial for X-linked SCID, although engraftment of transduced HSCs was low, as evidenced by the low gene marking in myeloid cells, patients demonstrated near-complete repopulation with genetically modified T lymphocytes (5). In vivo selective survival advantage of lymphocytes carrying the therapeutic transgene (the IL-2 common γ–receptor chain, encoded by *Il2rg*) contributed substantially to clinically beneficial levels of genetically corrected lymphocytes after gene therapy. These results strongly suggest that providing an in vivo selective advantage to transduced cells may be an attractive method of enhancing the repopulation of transduced cells in vivo. However, for most blood disorders, there will be no constitutive selective advantage of the gene-corrected cells.

One potential approach to in vivo selection of transduced HSCs is to incorporate drug resistance genes to convey protection against chemotherapeutic agents (6). Successful in vivo selection was previously documented in murine HSC transplantation models using several drug resistance genes, including multidrug resistance protein–1 (MDR-1; refs. 7, 8), dihydrofolate reductase (DHFR; ref. 9), and O^6-methylguanine-DNA methyltransferase (MGMT; refs. 10–12). However, in more clinically relevant large-animal models, in vivo selection using DHFR (13) and MDR-1 (14, 15) was variable and transient, with levels of gene-modified cells returning to baseline within a few weeks. MGMT is one of the most promising drug resistance genes that encodes for the DNA repair protein O^6-alkylguanine-DNA-alkyl-transferase (AGT). This protein confers resistance to the cytotoxic effects of alkylating agents, including nitrosoureas [e.g. 1,3-bis-(2-chloroethyl)-1-nitrosourea (BCNU)] and temozolomide (TMZ). To allow hematopoietic

Authorship note: Andre Larochelle, Uimook Choi, and Yan Shou contributed equally to this work.

Conflict of interest: The authors have declared that no conflict of interest exists.

Nonstandard abbreviations used: ANC, absolute neutrophil count; BCNU, 1,3-bis-(2-chloroethyl)-1-nitrosourea; BG, O^6-benzylguanine; CAG, cancer-associated gene; HOXB4, homeobox B4; IS, integration site; LAM-PCR, linear amplification–mediated PCR; LTR, long-terminal repeat; MGMT, O^6-methylguanine-DNA methyltransferase; MGMT*, MGMT P140K; MSCV, murine stem cell virus; P2A, 2A peptide from porcine teschovirus–1; PB, peripheral blood; T2A, 2A peptide from thosea asigna virus; TMZ, temozolomide; YFP, yellow fluorescent protein.

Citation for this article: *J. Clin. Invest.* **119**:1952–1963 (2009). doi:10.1172/JCI37506.

selection, O^6-benzylguanine (BG) is coadministered with TMZ for inactivation of endogenous MGMT activity. Several mutant forms of MGMT that give rise to altered AGT are highly resistant to inactivation by BG, but retain their ability to repair DNA damage (16, 17). The most commonly used mutant is MGMT P140K (MGMT*), which is almost completely resistant to BG, yet has a modest reduction in the rate of DNA adduct repair compared with wild-type AGT. This mutant form of MGMT can be incorporated in the gene transfer retroviral vectors to facilitate a greater selective advantage for primitive hematopoietic cells containing the vector. In vivo selection of HSCs using MGMT* was successfully achieved in murine (10–12) and canine models (18–20) and in human NOD/SCID-repopulating cells (21, 22). The same approach has also been proposed as a means to protect patients against dose-limiting hematopoietic toxicity following administration of chemotherapy combining alkylating agents and BG for the treatment of brain tumors (23). Protection of the BM compartment would allow administration of increased doses of chemotherapy agents to effect an improved therapeutic response.

A second approach to achieving therapeutic levels of gene-corrected cells is to confer a selective growth advantage upon gene-transduced cells. Homeobox B4 (*HOXB4*) is a potent stem cell self-renewal gene. In murine transplantation models, overexpression of HOXB4 has previously been shown to induce ex vivo expansion and self renewal of HSCs without compromising differentiation or homeostatic regulation of HSC pool size in murine transplantation models (24–26). More recently, HOXB4 function was examined in a clinically relevant nonhuman primate transplantation model: HOXB4 overexpression in rhesus $CD34^+$ cells was able to expand short-term repopulating cells, but had a less pronounced effect on long-term repopulating cells (27).

Drug resistance gene–mediated in vivo selection can amplify the percentage of gene-transduced HSCs; however, it is accompanied by a decrease in the overall number of HSCs. In murine transplantation studies, this limitation can be overcome by coexpressing HOXB4 with the drug resistance gene to allow selective regeneration of transduced cells after treatment with cytotoxic drugs (28). In this study, we examined the effects of an MGMT*-mediated drug-resistant system with or without an HOXB4-mediated HSC self-renewal system in transplanted rhesus macaques. Our findings indicate that in vivo chemoprotection of progenitor cells occurred, but selection of long-term repopulating HSCs was not seen.

Results

$CD34^+$ cells transduced with MGMT lentiviral vectors show transient chemoprotection after in vivo treatment with BG and TMZ.* We investigated whether in vivo chemoprotection could be achieved after transduction with MGMT*-expressing lentiviral vectors based on SIV and autologous transplantation of mobilized peripheral blood (PB) or BM $CD34^+$ cells in 5 rhesus macaques (Table 1). Gene transfer efficiency in the $CD34^+$ cell population before transplant in rhesus macaques varied between 18% and 53%, as determined by flow cytometry (Table 1).

In a first set of experiments, AMD3100-mobilized PB $CD34^+$ cells from animals RQ4876 and RQ4795 were transduced using SIV vectors expressing GFP-MGMT* fusion protein (Figure 1A). We administered 2 daily doses of 500 cGy total body irradiation before infusion of 5.6–6.4 × 10^6 $CD34^+$ cells/kg. Hematopoietic recovery was documented between 7 and 17 days (Table 1). At 3–6 months after transplant, each animal received the first of 4 successive BG/

Table 1
Reconstitution of irradiated rhesus macaques with transduced, autologous $CD34^+$ cells

Animal no.	$CD34^+$ cell source	Lentiviral vector[A]	$CD34^+$ cell transduction	Infusion dose (cells/kg)	ANC exceeding 500/μl (d)	In vivo treatment (no. cycles) BG/TMZ[B]	BG/BCNU[C]	In vivo selection[D]	Toxicity
MGMT* vector									
RQ4876	AMD3100-mobilized PB apheresis	GFP-MGMT*	50%	6.4 × 10^6	7	4	3	Transient	Death, pulmonary
RQ4795	AMD3100-mobilized PB apheresis	GFP-MGMT*	27%	5.6 × 10^6	17	4	0	Transient	Alive
RQ4513	G+S-mobilized PB apheresis	MGMT*-YFP	24%	6.7 × 10^6	11	2	2	Transient	Death, pulmonary GI
RQ4099	G+S-mobilized PB apheresis	MGMT*-YFP	18%	8.5 × 10^6	11	1	0	Transient	Death, radiation induced
RQ4152	G+S-mobilized BM	MGMT*-GFP	53%	2.1 × 10^6	8	7	1	Transient	Death, GI
MGMT*-HOXB4-GFP vector									
RQ4513	G+S-mobilized PB apheresis	MGMT*-HOXB4-GFP	20%	6.7 × 10^6	11	2	2	Transient	Death, pulmonary GI
RQ4099	G+S-mobilized PB apheresis	MGMT*-HOXB4-GFP	15%	6.7 × 10^6	11	1	0	Transient	Death, radiation induced
RQ4152	G+S-mobilized BM	MGMT*-HOXB4-GFP	50%	1.6 × 10^6	8	7	1	Transient	Death, GI

Animals RQ4876 and RQ4795 received cells transduced with MGMT* vectors: animals RQ4513, RQ4099, and RQ4152 received cells transduced with MGMT* or MGMT*-HOXB4-GFP vectors in a competitive repopulation setting (outcome data are repeated for the same animal). [A]All lentiviral vectors were amphotropic and had SIV envelope. [B]For RQ4876 and RQ4795, BG and TMZ concentrations were 120 and 245 mg/m^2, respectively. For RQ4513, RQ4099, and RQ4152, BG concentration was 120 mg/m^2 and TMZ concentration was in escalating doses: 170, 202, 230, 284, 325, 365, and 450 mg/m^2. [C]For all animals, BG and BCNU concentrations were 120 and 20 mg/m^2, respectively. [D]Includes both lymphoid and myeloid selection.

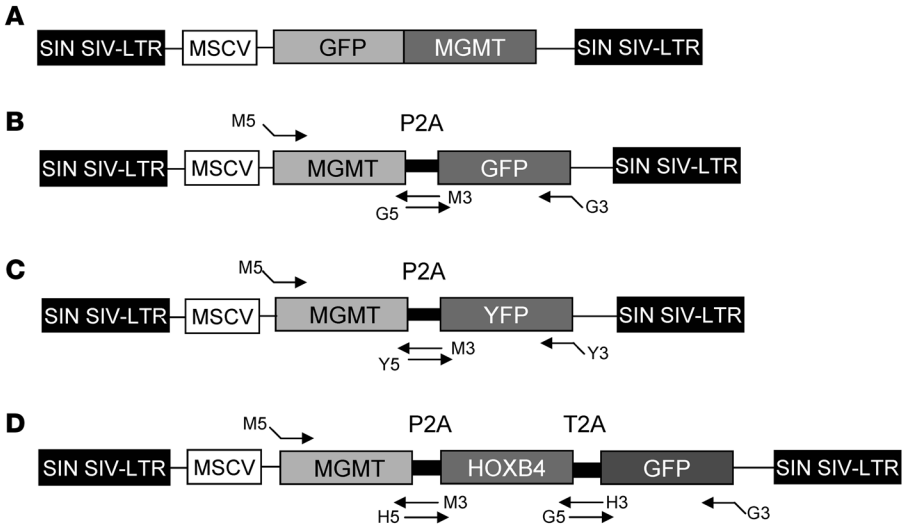

Figure 1

Vector constructs. (**A**) For the GFP-MGMT* SIV-based lentiviral vectors, expression of a GFP-MGMT* fusion gene was driven by the promoter activity of the MSCV LTR. (**B** and **C**) For MGMT*-P2A-GFP (**B**) and MGMT*-P2A-YFP (**C**) SIV vectors (referred to herein as MGMT*-GFP and MGMT*-YFP, respectively), P2A was used to generate a multicistronic expression cassette inserted in the pCL20cSLFR MSCV-GFP backbone. The primer pairs (M3, M5, Y3, Y5, G3, and G5) used for construction of the vectors are described in Methods. (**D**) For MGMT*-P2A-HOXB4-T2A-GFP SIV vectors (referred to herein as MGMT*-HOXB4-GFP), T2A was used to generate a multicistronic expression cassette inserted in the pCL20cSLFR MSCV-GFP backbone. MGMT*, HOXB4, and GFP were amplified and 2A-tagged from their respective cDNAs using primer pairs M5, M3, H5, H3, G5, and G3 as described in Methods.

TMZ treatments given at 1- to 2-month intervals. Substantial myelosuppression was seen in both animals after drug administration (Figure 2A).

Animal RQ4876 showed a rapid increase in transduced PB cells of all lineages in vivo after drug treatment. Steady-state marking levels of 2%, 6%, and 5% in granulocytes, lymphocytes, and monocytes, respectively, increased to peak levels of 52%, 33%, and 36% in the respective lineages after the first (granulocytes), second (lymphocytes), or third (monocytes) dose of BG/TMZ. The fourth dose of BG/TMZ led to only moderate increases in GFP^+ cells in all lineages. Treatment with BG/TMZ was well tolerated, with little to no cumulative toxicity. The proportion of GFP^+ cells subsequently declined gradually over a period of 200 days after the last BG/TMZ administration; marking levels in PB stabilized to values similar to those observed at steady state before the first treatment with BG/TMZ, with 2% GFP^+ granulocytes, 6% GFP^+ lymphocytes, and 3% GFP^+ monocytes (Figure 2B). Lentiviral vector provirus copy numbers were also determined by real-time PCR at several time points in DNA from PB (data not shown). Overall, there was a good correlation between flow cytometry and real-time PCR results, which suggests that on average, repopulating cells contained no more than 1 vector copy and that gene silencing was not responsible for the gradual decrease in gene marking levels in vivo.

Animal RQ4795 had very low steady-state gene marking levels in PB granulocytes (0.1%), lymphocytes (0.01%), and monocytes (0.2%; Figure 2B). We tested the safety and feasibility of improving very low baseline gene marking levels with in vivo infusion of BG/TMZ. No change in GFP^+ granulocytes was detected at any time point after BG/TMZ administration. A peak increase in GFP^+ lymphocytes (0.2%) and monocytes (1.5%) was observed after the second dose of BG/TMZ, but the increase was only transient, returning to baseline levels within 30 days. The third and fourth doses of BG/TMZ resulted in substantial myelosuppression, but had no impact on gene marking levels in any lineage.

In a second set of experiments, we tested whether alternative SIV MGMT*-expressing vectors in combination with minor modifications to transduction conditions and escalating doses of TMZ could result in improved longer-term gene marking levels. Rhesus competitive repopulation experiments were set up using equal numbers of mobilized PB or BM $CD34^+$ cells transduced with SIV vectors expressing MGMT* alone (containing GFP or yellow fluorescent protein [YFP]) or MGMT*-HOXB4-GFP (see Methods and Figure 1). Multicistronic cassettes containing GFP or YFP were generated in each vector using the 2A peptide from porcine teschovirus–1 (P2A) and thosea asigna virus (T2A) (Figure 1, B–D). All 3 animals in this study — RQ4513, RQ4099, and RQ4152 — were mobilized with G-CSF plus SCF and received 2- to 3-fold more $CD34^+$ cells/kg compared with the AMD3100-mobilized animals RQ4876 and RQ4795 after total body irradiation conditioning (Table 1). Hematopoietic reconstitution was rapid, with the absolute neutrophil count (ANC) reaching 500 cells/μl or more by 8–11 days after transplant. All animals showed a total of 3%–6% marked PB granulocytes and monocytes, and 1%–12% marked PB lymphocytes, at 60 days after transplant (Figures 3, 4, 5). After stable engraftment, we evaluated the drug combination BG/TMZ. The dose of BG was fixed at 120 mg/m^2, but, in contrast to animals RQ4876 and RQ4795, the dose of TMZ was gradually escalated from 170 to 450 mg/m^2/d for a 5-day period. All animals showed significant myelosuppression after each treatment (Supplemental Figure 1; supplemental material available online with this article; doi:10.1172/JCI37506DS1).

The first animal in this group, RQ4513, was treated with 2 courses of BG/TMZ at 12 and 15 weeks after transplant. The ANC nadirs were 780 cells/μl at day 16 after the first treatment and 210 cells/μl at day 14 after the second treatment. The percentage of GFP^+ and YFP^+ granulocytes (Figure 3A) and monocytes (Figure 3C) increased from 4% to 40% (YFP) and 4% to 50% (GFP), but gradually declined back to 4% (GFP) and 10% (YFP) over a period of 50 days after the second dose of BG/TMZ. The absolute number of YFP-transduced granulocytes increased from 40 cells/μl before drug treatment to approximately 200 cells/μl after 2 courses of BG/TMZ, which suggests that YFP-transduced $CD34^+$ cells were protected and expanded after BG/TMZ treatment (Figure 3B). Similarly, the percentage of GFP^+ and YFP^+ lymphocytes doubled after the second BG/TMZ administration, but GFP^+ lymphocytes rapidly declined back to pretreatment levels (Figure 3D).

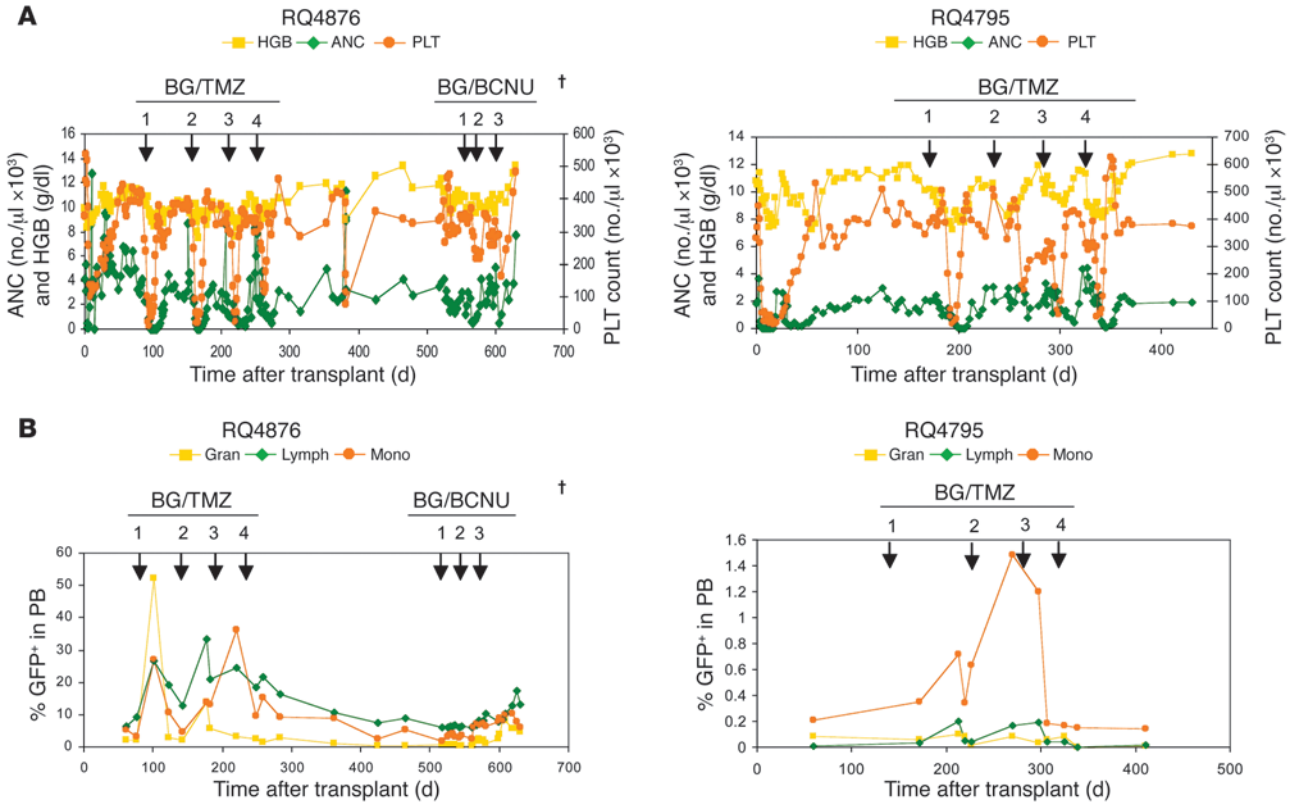

Figure 2

In vivo selection in SIV-transduced animals RQ4876 and RQ4795 after multiple cycles of BG/BCNU and/or BG/TMZ. Both animals were transplanted with CD34⁺ cells transduced with lentiviral GFP-MGMT* vector. (**A**) ANC, hemoglobin (HGB), and platelet (PLT) counts in PB over time for RQ4876 and RQ4795. (**B**) Percent GFP⁺ granulocytes (Gran), lymphocytes (Lymph), and monocytes (Mono) from PB for RQ4876 and RQ4795. Arrows denote cycles of drug administration; "†" indicates time of animal death.

The second animal, RQ4099, was treated with a single course of BG/TMZ at week 10 after transplant. The ANC nadir was 190 cells/μl at day 14 after treatment. The percentage of GFP⁺ and YFP⁺ granulocytes and monocytes increased from a steady-state level of 3%–5% to a peak of 25%–30%, but returned to baseline gene marking levels within 50 days after BG/TMZ administration (Figure 4A). In vivo enrichment of GFP⁺ and YFP⁺ B cells was also transient (Figure 4B). In T cells, GFP and YFP marking levels were 1% at steady state and peaked at 13% (GFP) and 23% (YFP) after BG/TMZ treatment. The proportion of gene marked T cells subsequently declined and stabilized at 4% (GFP) and 5% (YFP) (Figure 4B). The animal died approximately 3 months after BG/TMZ treatment due to pulmonary fibrosis. This complication is occasionally seen in animals not treated with BG/TMZ and is likely secondary to radiation received as a conditioning regimen prior to transplant.

The third animal, RQ4152, had pretreatment gene marking levels of 5% in granulocytes, 3% in monocytes, 10% in B cells, and 1% in T cells. The animal was treated with 7 courses of BG/TMZ, with TMZ doses ranging from 170 to 450 mg/m²/d. The ANC nadir was 850 cells/μl at day 6 after the first treatment (170 mg/m² TMZ) and 7 cells/μl at day 9 after the last treatment (450 mg/m² TMZ). After each course of drug treatment, there was a rapid increase in GFP marking in all lineages. The highest marking achieved after the last course of BG/TMZ treatment was 94% for myeloid cells and 57% for lymphoid lineages (Figure 5A). The proportion of GFP⁺ cells subsequently declined and leveled off at 10% for granulocytes, 5% for monocytes, 17% for B cells, and 30% for T cells at 150 days after the last treatment (Figure 5A). Correspondingly, the absolute number of transduced granulocytes increased after each drug treatment with, for example, levels of 80 cells/μl before the fourth course peaking to 698 cells/μl after the seventh course and stabilizing at approximately 250 cells/μl (Figure 5B). These results indicate that MGMT*-transduced cells were protected and expanded following multiple courses of BG/TMZ treatments with TMZ dose escalation up to 450 mg/m². In pediatric patients, the maximum tolerated dose of TMZ without BG is 185 mg/m² (29); therefore, gene therapy resulted in substantial dose escalation due to protection from hematopoietic toxicity. As shown by pharmacokinetic data (Table 2), the absorption and clearance of TMZ in animal RQ4152 at the time of the seventh dose of TMZ was comparable to that seen in treated pediatric patients. Moreover, the AUC for TMZ was about 2-fold greater than that seen in pediatric patients (Table 2), confirming that BM protection was achieved against BG/TMZ by MGMT* overexpression in this animal. This is particularly interesting given that BG is known to significantly enhance TMZ toxicity, necessitating TMZ dose reductions (30). Given the relative lack of nonhematopoietic toxicity seen in our series with BG/TMZ, we conclude that hematopoietic protection via transfer of MGMT* allows for substantial dose escalation and administration of repeated drug courses.

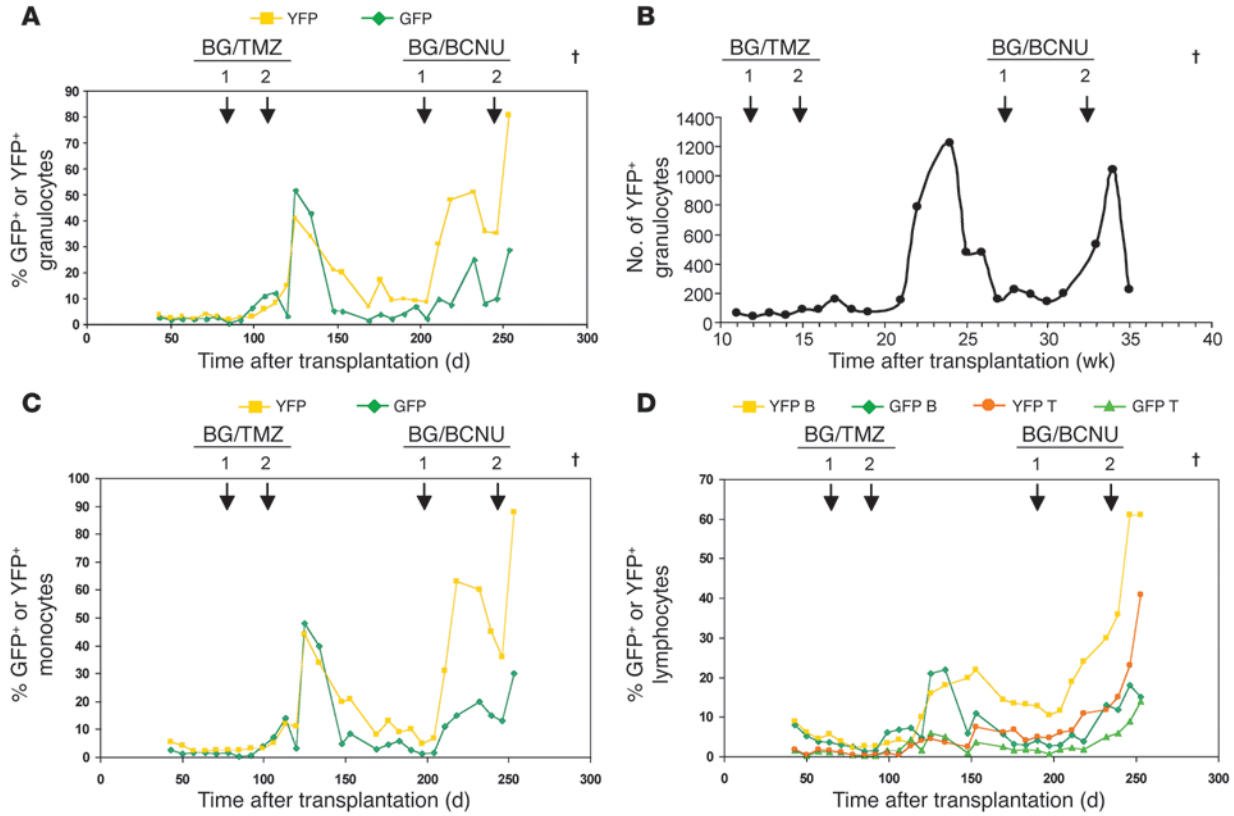

Figure 3

In vivo selection in SIV-transduced animal RQ4513 after 2 cycles of BG/TMZ and 2 cycles of BG/BCNU. Rhesus competitive repopulation experiments were set up using equal numbers of mobilized PB CD34+ cells transduced with SIV vectors expressing MGMT*-YFP or MGMT*-HOXB4-GFP. (**A**) Percent GFP+ and YFP+ granulocytes from PB. (**B**) Absolute number of YFP+ granulocytes. (**C**) Percent GFP+ and YFP+ monocytes from PB. (**D**) Percent GFP+ and YFP+ B cells and T cells from PB. Arrows denote cycles of drug administration; "†" indicates time of animal death.

Polyclonal hematopoiesis is sustained after BG/TMZ treatment. The clonal composition before and after BG/TMZ treatment was analyzed by linear amplification–mediated PCR (LAM-PCR) in animals RQ4152 and RQ4513, which showed the highest in vivo gene marking levels. DNA isolated from PBLs before and after 1, 2, 6, and 7 courses of BG/TMZ was used for LAM-PCR. Gel electrophoresis showed contribution of multiple clones at all time points analyzed (Supplemental Figure 2). Individual bands from LAM-PCR products were picked from the gel and sequenced directly after PCR amplification. Using previously described selection criteria (31), we retrieved and analyzed 254 independent unequivocal retroviral integration sites (ISs; 152 for RQ4152, Supplemental Table 1; and 102 for RQ4513, Supplemental Table 2). The majority of these ISs occurred within transcription units, mainly within introns (Table 3), consistent with data from previous reports (31–33). Also, in agreement with previously published data (31–33), SIV integration events did not favor locations upstream or downstream of transcription units (Table 3), indicating no preference for integration near transcription start sites. In animals RQ4152 and RQ4513, 7.9% and 3.9% of ISs identified, respectively, were in or near cancer-associated genes (CAGs; Table 3 and Supplemental Tables 1 and 2). We identified 8 clones that appeared repetitively before and after drug treatment, which suggests that the same clones contributed to hematopoiesis after in vivo selection with BG/TMZ.

In vivo treatment with BG/BCNU does not result in long-term chemoprotection and causes high levels of nonhematopoietic toxicity. In animals RQ4876, RQ4513, and RQ4152, which showed evidence of increased gene marking after multiple BG/TMZ treatments, we tested whether chemoprotection could be achieved using BCNU as an alternative alkylating agent. Several months after the last dose of BG/TMZ, we administered 1–3 successive infusions of 120 mg/m^2 BG and 20 mg/m^2 BCNU (hereafter referred to as BG/BCNU). In animal RQ4876, a moderate but steady increase in marking levels was seen after each BG/BCNU dose. Pretreatment levels of 2% in granulocytes, 6% in lymphocytes, and 5% in monocytes peaked at 9%, 17%, and 10%, respectively, after the third dose (Figure 2B). BG/BCNU treatment also resulted in a rapid increase in GFP/YFP marking in all hematopoietic lineages in animal RQ4513, with maximal levels of 90% in granulocytes and monocytes, 60% in B cells, and 40% in T cells (Figure 3). A more modest effect was seen in animal RQ4152 (Figure 5).

All animals that received BG/BCNU eventually developed substantial nonhematopoietic toxicity, in contrast to what was seen using BG/TMZ. RQ4876 developed severe tachypnea, fevers, and failure to thrive with weight loss 1 month after the third dose of BG/BCNU. X-rays revealed diffuse pulmonary infiltrates consistent with pneumonitis (Supplemental Figure 3A). Euthanasia was performed 35 days after the last administration of BG/BCNU. Animal RQ4513 developed severe pulmonary and

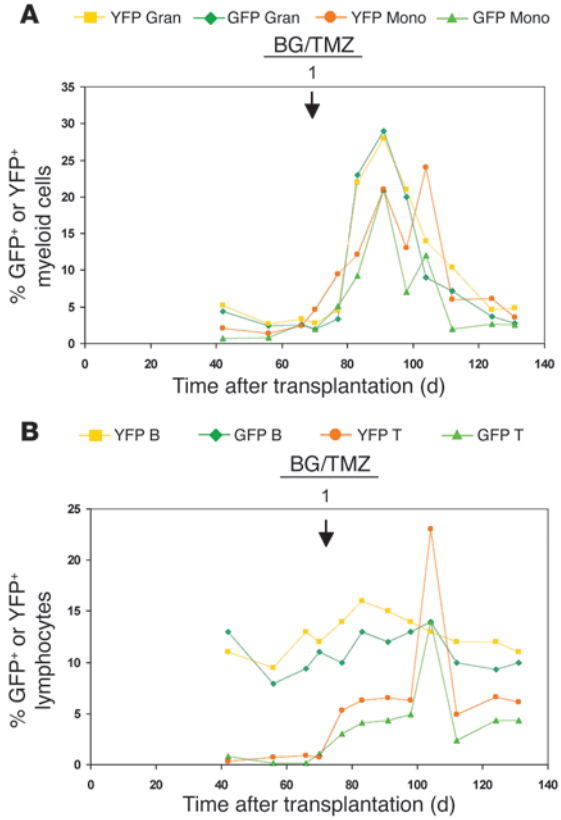

Figure 4
In vivo selection in SIV-transduced animal RQ4099 after 1 cycle of BG/TMZ. Rhesus competitive repopulation experiments were set up using equal numbers of mobilized PB CD34+ cells transduced with SIV vectors expressing MGMT*-YFP or MGMT*-HOXB4-GFP. (**A**) Percent GFP+ and YFP+ granulocytes and monocytes from PB. (**B**) Percent GFP+ and YFP+ B cells and T cells from PB. Arrows denote cycles of drug administration.

gastrointestinal complications, and euthanasia was performed 2 weeks after the second cycle of BG/BCNU. Specimens collected at necropsy revealed extensive pulmonary edema and widespread colonic necrosis with pseudomembrane formation (Supplemental Figure 3B). Animal RQ4152 was clinically well after receiving 7 courses of BG/TMZ, but developed severe gastrointestinal complications and died 7 days after 1 course of BG/BCNU. At necropsy, specimens were consistent with a diagnosis of severe necrohemorrhagic colitis (Supplemental Figure 3C). While lower doses of BCNU may have been less toxic, we observed no significant decrease in complete blood count and no change in vector marking levels when a single test dose of 5 mg/m^2 was administered in animal RQ4876 (data not shown).

Because all animals were euthanized shortly after BG/BCNU administration, long-term persistence of improved marking levels could not be assessed. In the BCNU-treated animal RQ4876, follow-up was possible for a slightly longer period of time after BCNU administration (about 80 days); in this animal, a clear trend down in marking levels was evident at the time of euthanasia (Figure 3B), which suggests a lack of persistent chemoprotection with BCNU, as was seen after TMZ administration.

Absence of long-term chemoprotection in vivo is not caused by lack of transduction of long-term repopulating HSCs. We investigated whether the lack of stable selection in vivo could be the result of poor transduction of long-term repopulating HSCs. Several lines of evidence indicated transduction of HSCs. First, in all animals, persistence of substantial expression of the GFP transgene in T cells, B cells, granulocytes, and monocytes for several months after transplant was an indication of HSC transduction (Figure 2B and Figures 3–5). Second, in animal RQ4876, 10% of CD34+ cells isolated from the BM 630 days after transplant were GFP+, as assessed by flow cytometry (data not shown). Third, we also obtained molecular evidence of transduction of HSCs in animal RQ4876. Using DNA isolated from the BM of this animal more than 1 year after transplant, we performed LAM-PCR and isolated 10 ISs. Demonstration of common lentiviral ISs in sorted subpopulations of the PB (T cells, B cells, and granulocytes) collected before BG/TMZ treatment (day 60 after transplant), after the last dose of BG/TMZ (day 374), and after the last dose of BG/BCNU (day 630) was performed by PCR using 1 vector long-terminal repeat (LTR) primer and 1 genomic primer spanning a region of each IS. We were able to detect 2 common ISs (Figure 6), providing a clear demonstration of the transduction of HSCs contributing in the long term to the different hematopoietic lineages. Interestingly, of the 2 common ISs, the one designated IS 1 (Figure 6) was undetectable prior to drug treatment, but its contribution to all lineages increased over time after BG/TMZ and BG/BCNU treatment, a characteristic of HSC dynamics. Overall, these observations rule out the lack of transduction of HSCs as a possible mechanism for the absence of long-term chemoprotection. Given the consistent data among the 5 animals described in the present study, we believe that these conclusions can be generalized to all animals.

HOXB4 does not confer HSC amplification in the rhesus macaque transplant model. HOXB4 is a potent HSC amplifier in murine transplantation models. In our competitive rhesus transplantation model, we investigated whether HOXB4 could improve engraftment of transduced HSC and progenitor cells in animals RQ4513, RQ4099, and RQ4152 (Table 1). Gene transfer efficiencies in CD34+ cells were similar between MGMT* and MGMT*-HOXB4-GFP vectors before cell infusion based on flow and CFU analysis. For animals RQ4513 and RQ4099, the GFP/YFP ratio allowed direct measurement of competitive engraftment of MGMT*-HOXB4-GFP– versus MGMT*-transduced cells. In both animals, we observed a similar engraftment pattern. The initial engraftment levels for both MGMT*- and MGMT*-HOXB4-GFP–transduced granulocytes at 2 weeks after transplant were similar in RQ4513 (17% versus 13%; Supplemental Figure 4A) and RQ4099 (23% versus 25%; Supplemental Figure 4B). Marking levels gradually declined for both compartments before they stabilized at a similar level. In RQ4513, MGMT*-HOXB4-GFP marking stabilized at 2.6%, and MGMT* marking stabilized at 2.9%, in granulocytes 78 days after transplant (Supplemental Figure 4A). Marking levels in granulocytes in RQ4099 stabilized at 2.5% for MGMT*-HOXB4-GFP and 3.3% for MGMT* at 66 days after transplant (Supplemental Figure 4B). For animal RQ4152, because both MGMT* and MGMT*-HOXB4-GFP–transduced cells used GFP as an expression marker, Southern blot was used to distinguish the 2 compartments. Again, there was no difference in engraftment levels between MGMT*- and MGMT*-HOXB4-GFP–transduced cells (Supplemental Figure 4C, lane 1). Moreover, we did not observe any advantage for in vivo selection in the cells containing the MGMT*-HOXB4-GFP

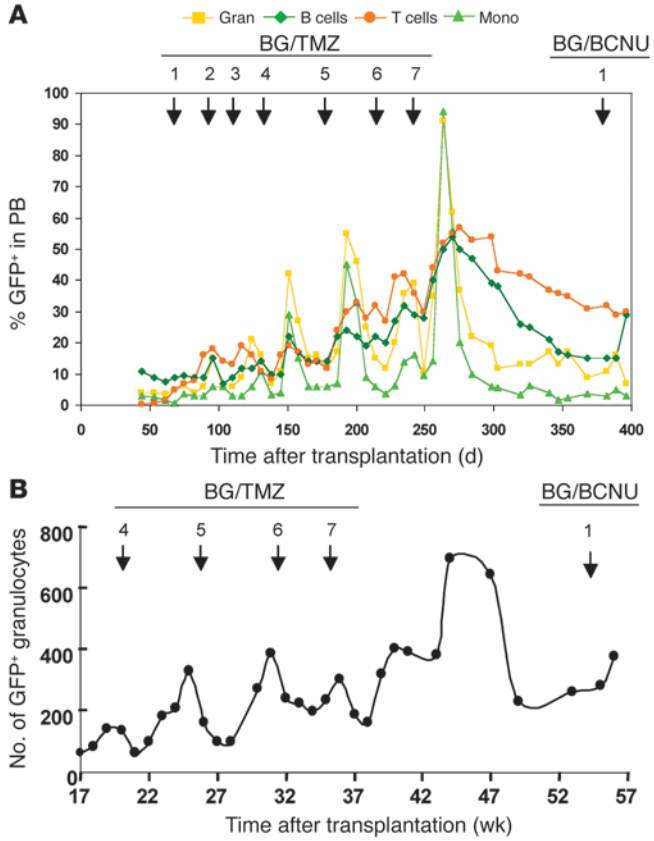

Figure 5
In vivo selection in SIV-transduced animal RQ4152 after multiple cycles of BG/TMZ and 1 cycle of BG/BCNU. Rhesus competitive repopulation experiments were set up using equal numbers of mobilized PB CD34+ cells transduced with SIV vectors expressing MGMT*-GFP or MGMT*-HOXB4-GFP. (**A**) Percent GFP+ granulocytes, B cells, T cells, and monocytes from PB for RQ4152. (**B**) Absolute number of GFP+ granulocytes. Arrows denote cycles of drug administration.

vector. For instance, in RQ4513 (Figure 3) and RQ4099 (Figure 4), marking levels in all lineages increased in parallel between MGMT*- and MGMT*-HOXB4-GFP–transduced cells after drug treatment. For RQ4152, there was also no difference in marking levels between MGMT*- and MGMT*-HOXB4-GFP–transduced cells after BG/TMZ treatment, as determined by Southern blot (Supplemental Figure 4C, lanes 2–5). At 8 months after transplant, HOXB4 expression was detected in MGMT*-HOXB4-GFP–marked PB cells sorted by flow cytometry (Supplemental Figure 5), which confirmed that the lack of amplification was not caused by absent expression of HOXB4.

Discussion

MGMT-mediated in vivo selection with lentiviral vectors occurs mainly in progenitor cells, not HSCs*. In the current study, we evaluated BG/TMZ and BG/BCNU for in vivo selection of CD34+ cells modified with MGMT* lentiviral vectors to increase transduced blood cells in the clinically relevant rhesus macaque model. We observed that 2 animals with pretreatment steady-state in vivo marking levels of 2% and 0.2% showed transient increase in GFP expression in both myeloid and lymphoid lineages after 4 cycles of BG/TMZ treatment, indicating in vivo MGMT* gene expression and chemoprotection of progenitor cells with transient repopulating capacity. Additionally, 3 other animals with higher baseline marking levels (5% in PB granulocytes) showed a more persistent, yet still transient, increase in gene-marked cells in vivo in lymphoid and/or myeloid lineages after BG/TMZ administration. Additional cycles of chemotherapy using BCNU as an alternative alkylating agent resulted in similar increases in gene marking levels.

Overall, these results indicate that the relatively high transduction efficiencies achieved in CD34+ cells using lentiviral vectors support chemoprotection of progenitor cells, but not long-term repopulating stem cells. Four mechanisms can be considered in accounting for the lack of stable selection at the stem cell level. First, we demonstrated that the absence of persistent chemoprotection did not relate to the lack of transduction of long-term repopulating HSCs. Detection of transgene expression in the long term (close to 2 years in 1 animal) after transplant in both lymphoid and myeloid lineages was an indication of transduction of long-term repopulating HSCs. In a prior study, 3 rhesus macaques — transplanted with CD34+ cells transduced using SIV vectors and conditions similar to those used in the present study — demonstrated significant vector marking and expression of the transgene for up to 4 years after transplant (34). In animal RQ4876 in the present study, 10% of CD34+ cells isolated from the BM at day 630 after transplant expressed the GFP transgene. More importantly, we demonstrated 2 common lentiviral ISs in sorted subpopulations of the PB (T cells, B cells, and granulocytes) of RQ4876 collected up to 630 days after transplant. Of the 2 common ISs (Figure 6), 1 had characteristics of HSC, not progenitor cell, dynamics with amplification over time after BG/TMZ and BG/BCNU treatment. Overall, these observations indicate transduction of HSCs contributing in the long term to the different hematopoietic lineages.

Second, in spite of the observed lack of selection with TMZ, it is possible that selection of HSCs could have been achieved with BCNU at doses lower than 20 mg/m^2, as toxicity prevented long-term follow-up. In animal RQ4876, we administered a lower dose of BCNU (5 mg/m^2), but no significant decrease in complete blood count and no change in vector marking levels was observed. While titrating the dose of BCNU may be possible in rhesus macaques for selection of transduced HSCs with decreased toxicity, it is unlikely that this drug could be used safely in patients for which individualized dose titration would not be possible.

Third, we considered the possibility that the lack of HSC selection could be related to the deleterious effect of high murine stem cell virus–driven (MSCV-driven) expression of MGMT* on cellular proliferation and engraftment, or, alternatively, to inadequate MGMT expression from this promoter in HSCs. As recently reported by Milsom and colleagues, while MGMT* expression by weaker cellular promoters (e.g., phosphoglycerate kinase) was sufficient for in vivo selection, viral promoter–driven high expression of MGMT* led to increased localization to the nucleus/chromatin, resulting in competitive repopulation defects in HSCs (35). However, the toxicity was observed with the SFFV viral promoter, causing a 10-fold higher level of MGMT* than with the MSCV promoter used in the present study. In addition, in our present study, MGMT* activity was sufficient to allow transient chemoprotection, but the low BG-noninhibitable activity detected in our transplanted animals (e.g., 7 fmol [^{3}H]-methylated protein/mg protein detected in RQ4876) suggested that the potential toxicity

Table 2
Pharmacokinetic study of RQ4152 after the seventh course of TMZ/BG treatment

Parameter	RQ4152	Pediatric population[A]
TMZ clearance (l/h/m^2)	5.4	4.9 (1.6–10.8)
C_{max} (mg/l)	24.6	9.1 (4.3–19.0)
T_{max} (h)	1.0	1.2 (0.2–2.9)
K_a (h^{-1})	1.6	2.4 (0.1–31.6)
TMZ AUC value (μg/ml•h)	65.1	37.7 (18.6–120.3)
MTIC AUC value (μg/ml•h)	1.9	1.0 (0.1–2.1)

C_{max}, maximum concentration; T_{max}, maximum time; K_a, absorption rate constant; MTIC, 3-methyl-(triazen-1-yl)imidazole-4-car-boxamide, an active species to which TMZ is spontaneously hydrolyzed at physiologic pH. [A]Mean (range) in a pediatric population receiving approximately 185 mg/m^2 TMZ (29).

of high MGMT* expression from the lentiviral constructs we used is an unlikely explanation for the lack of stable enrichment of gene modified cells in rhesus macaques.

In contrast, the internal MSCV promoter used in the present study, although active in the rhesus CD34$^+$ progenitor cells and blood progeny, may have not provided adequate expression of the MGMT* transgene in HSCs. The MSCV promoter was chosen at the outset of these experiments based on our extensive experience with it in the murine system, where we have previously shown it to be active in HSCs (36–38). Interestingly, a recent study showed that while the MSCV LTR is expressed in undifferentiated mouse ES cells, it has much lower transcriptional activity than that of the human elongation factor–1α (EF1α) promoter or the hybrid CAG promoter (CMV enhancer, chicken β-actin promoter and intron, and globin polyadenylation signal; ref. 39). In the context of self-inactivating (SIN) HIV-based lentiviral vectors, the EF1α promoter gave about a 6-fold increase in expression relative to that of the MSCV LTR, as judged by GFP fluorescence, while the CAG vector gave 2- to 3-fold better expression (39). The promoter MND may also offer advantages for expression in HSCs. It includes deletion of the negative control region in the 5′ region of the U3 portion of the LTR, and it contains 2 copies of the 72-bp enhancer repeat, compared with 1 copy in MSCV (40–43). Another promoter with potential activity in HSCs is the ubiquitin-C promoter. SIN lentiviral vectors using this promoter to drive GFP expression were previously found to express well in the primitive embryonic blastula cells of mice after injection of vector into single-cell embryos (44). Together, these data raise the possibility that either of the latter regulatory elements may provide better expression than the MSCV promoter in HSCs, thus allowing better long-term in vivo selection.

Fourth, the lack of selection at the stem cell level may be attributed to the ability of untransduced stem cells to resist the cytotoxic effects of TMZ. The cytotoxicity of TMZ is largely attributed to the induction of single-strand methyl adducts at the O^6 position of guanines, leading to mispairing with thymidine residues. When TMZ-treated cells divide, DNA replication is inhibited, triggering apoptosis and cell death. In contrast to rapidly dividing progenitor cells, HSCs cycle slowly in vivo in large animals (once per 23–36 weeks at steady state; ref. 45); therefore, the TMZ-induced O^6-methylguanine DNA adducts may persist longer in these cells with no deleterious effects. During this period of quiescence, in the absence of BG, endogenous MGMT levels would be expected to recover, leading to repair of O^6-methylguanine DNA adducts in both transduced and untransduced HSCs. When the untransduced HSCs eventually divide, the TMZ-induced DNA lesions may have been repaired, preventing the cells from undergoing apoptosis. Given the marked differences in estimates of the average HSC replication rate between mice (once per 2.5 weeks; refs. 45, 46) and large animals (once per 23–36 weeks; ref. 45), the same reasoning could also explain why in vivo selection of HSCs using MGMT* was successfully achieved in mice (10–12). In our rhesus macaque study, BG was given once daily for 5 days; perhaps continuous administration of BG for a longer period of time could have prevented recovery of endogenous MGMT in slowly dividing HSCs and allowed for a stable increase in gene marking levels in vivo. Another option would be to design a treatment protocol that forces HSC cycling using appropriate hematopoietic cytokines during the period of cytotoxic drug treatment.

An alternative explanation for the increased resistance of untransduced HSCs to BG inactivation may be related to higher levels of endogenous MGMT compared with more mature progenitor cells. Indeed, high levels of expression of molecules such as ABCG2, MDR-1, and ALDH in HSCs (47–50) are postulated to be of importance in protecting HSCs from genotoxic or metabolic damage. Moreover, in highly purified murine long-term repopulating HSCs (defined as CD34$^-$Lin$^-$c-Kit$^+$Sca1$^+$), MGMT expression was 2–3 times higher than that present in more mature progenitor cells (defined as Lin$^-$c-Kit$^+$Sca1$^-$), as determined previously by query of a GEO DataSet Browser for microarray data of MGMT expression in hematopoietic cells (51). Optimization of inhibition of endogenous HSC MGMT through a pharmacokinetic and pharmacodynamic approach could improve in vivo selection in HSCs.

BG/BCNU has more nonhematopoietic toxicity than does BG/TMZ for MGMT-mediated in vivo selection.* An important consideration regarding the ultimate use of the MGMT* selection system in humans is whether it can be used with acceptable toxicity. In our rhesus macaque study, euthanasia was performed in 3 of 3 (100%) animals that received BG/BCNU. In contrast, animal RQ4795 survived treatment with BG/TMZ alone without complications, and animal RQ4099, also treated with BG/TMZ alone, was euthanized following complications attributed to radiation-induced pulmonary fibrosis. These observations indicate a higher toxicity of the alkylating agent BCNU compared with TMZ. Gastrointestinal complications were observed with BCNU, including necrohemorrhagic colitis in animal RQ4152 and colonic necrosis with pseudomembrane formation in animal RQ4513. Pulmonary complications were also seen in 2 animals, including pulmonary congestion/edema (RQ4513) and infections (RQ4876). These complications have never or only rarely been detected in more than 200 transplanted rhesus macaques at

Table 3
IS distribution and association with CAGs for RQ4152 and RQ4513

Parameter	RQ4152	RQ4513
Transcription units	70%	77%
Introns	64%	71%
Exons	6%	6%
Within 10 kb upstream of gene	4.6%	3.9%
Within 10 kb downstream of gene	2.6%	3.9%
In or near CAGs	7.9%	3.9%

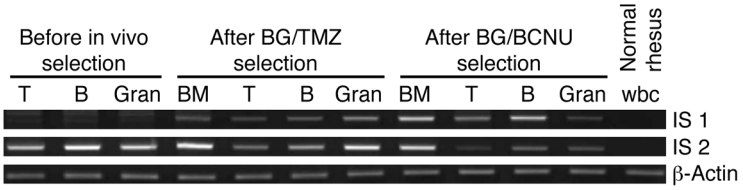

Figure 6
Transduction of long-term repopulating rhesus macaque HSCs with lentiviral vectors. Using DNA isolated from the BM of rhesus macaque RQ4876 more than 1 year after transplant, we performed LAM-PCR and isolated 10 ISs. Demonstration of common lentiviral ISs in sorted subpopulations of the PB — T cells, B cells, and granulocytes — collected before and after BG/TMZ or BG/BCNU selection was subsequently performed by PCR using 1 vector LTR primer and 1 genomic primer spanning a region of each IS. We detected 2 common ISs, providing a clear demonstration of the transduction of HSCs contributing in the long term to the different hematopoietic lineages. DNA extracted from wbcs of a nontransplanted animal was used as a negative control. Each DNA sample was amplified using β-actin–specific primers as a positive control.

our institutions, which suggests that they are causally related to the administration of BG/BCNU. In contrast, TMZ toxicity was highly specific for hematopoietic cells, and multiple courses were well tolerated without cumulative or nonhematopoietic toxicity.

HOXB4 does not provide a proliferative advantage to transduced long-term repopulating cells. In addition to drug resistance genes for selection of transduced cells after transplantation, retroviral vectors armed with genes that give a proliferative advantage to the transduced cells have also been proposed to improve in vivo gene marking levels (28). Genes that favor self renewal of HSCs have been prime candidates to promote selective growth advantage of transduced HSCs for improved gene therapy. One particular transcription factor, HOXB4, has been extensively studied as a way of increasing the self renewal of HSCs and hematopoietic progenitor cells in mice (24, 25, 52), humans, and large animal models (27) both in vivo and in vitro.

In our primate competitive repopulation assay, we transduced monkey CD34$^+$ cells with either a MGMT*-HOXB4-GFP vector or a vector expressing only the MGMT* gene and analyzed the competitive repopulating ability of these cells in vivo. We found no substantial difference in engraftment levels between MGMT*- and MGMT*-HOXB4-GFP–transduced cells both before and after chemotherapy treatment up to 400 days after transplant. Our data are consistent with those of Zhang, Kiem, and colleagues, who found that, in contrast to mouse studies, no significant advantage for the HOXB4-transduced cells was observed in the long term after transplant in a similar nonhuman primate competitive study (27). The same group also recently reported what we believe to be the first instances of leukemia linked to HOXB4 expression, both in the original group of monkeys now followed longer term and in dogs that received cells transduced with a HOXB4-expressing retroviral vector (53). Some 2 years after transplant, 3 of 4 animals (2 of 2 dogs and 1 of 2 nonhuman primates) developed acute myeloid leukemias, and several lines of evidence have strongly implicated HOXB4 in leukemogenesis (53). In animal RQ4152, euthanized as a result of complications of BG/BCNU treatment, we demonstrated by direct sequencing no occurrence of monoclonality, at least over the period of observation of approximately 12 months.

MGMT lentiviral vectors can be used for TMZ dose intensification.* TMZ is a chemotherapeutic alkylating agent with demonstrated efficacy for the treatment of malignant gliomas. A recent study by Stupp et al. revealed that TMZ in combination with radiation therapy yielded a statistically significantly greater prolongation of the survival time compared with radiation alone in patients with newly diagnosed gliomas (23). Increased doses of TMZ may lead to further increases in survival, but dose intensification is precluded because of increased toxicity. In the present study, we showed that BM protection was achieved by MGMT* overexpression after multiple courses of BG/TMZ treatments with TMZ dose escalation up to 450 mg/m^2, twice the maximum tolerated dose of TMZ in pediatric patients. This is potentially significant because the use of BG in patients to diminish MGMT activity and drug resistance in tumor cells has been associated with increased hematopoietic toxicity and has necessitated TMZ dose reductions (30). Our findings indicate that drug resistance in 5%–10% of myeloid progenitors allows for increased hematopoietic recovery and increased tolerance to TMZ. The transient chemoprotection observed in this study may be useful for patients with malignant brain tumors treated with both BG and TMZ dose intensification in order to overcome tumor cell drug resistance. While cumulative genotoxicity resulting from the combined use of alkylating agents (e.g., TMZ) and lentiviral vectors needs to considered, our study revealed no evidence of clonal dominance or leukemic transformation using this approach, at least over the period of observation covered.

Methods

Collection of PB HSCs from rhesus macaques. All 5 rhesus macaques (*Macaca mulatta*) used in these studies were housed and handled in accordance with the guidelines set by the Committee on Care and Use of Laboratory Animals of the Institute of Laboratory Animal Resources, National Research Council (DHHS publication no. NIH 85-23). Animals RQ4876 and RQ4795 were treated under a protocol approved by the Animal Care and Use Committee of the NHLBI. Animals RQ4513, RQ4099, and RQ4152 were housed in the Animal Resource Center of St. Jude Children's Research Hospital and were treated under a protocol approved by the St. Jude IACUC.

For stem cell mobilization, animals RQ4876 and RQ4795 were mobilized using a single subcutaneous dose of 1 mg/kg AMD3100 (Genzyme), and PB cells were collected by leukapheresis 3 hours after AMD3100 administration as described previously (54). The other 3 animals, RQ4513, RQ4099, and RQ4152, were given G-CSF at 10 μg/kg/d and SCF at 50 μg/kg/d (Amgen) through subcutaneous injection for 3 days and twice daily on day 4. For RQ4513 and RQ4099, mobilized PB cells were collected by leukapheresis on day 5 as described previously (55); for RQ4152, BM was aspirated from the posterior iliac crest. In animal RQ4152, BM was harvested after in vivo cytokine administration based on our previous observation that in vivo manipulation of HSCs prior to BM harvest can improve retroviral gene transfer into HSCs by promoting cell cycling and increasing receptor density in nonhuman primate models (56).

For each cell fraction (AMD3100-mobilized PB cells, G-CSF and SCF–mobilized PB cells, and BM), PBMCs were isolated using density gradient centrifugation over lymphocyte separation media (LSM; ICN Biomedicals/Cappel). CD34$^+$ cells were enriched using the 12.8 IgM anti-CD34 biotinylated antibody and MACS streptavidin microbeads (Miltenyi Biotec) per the manufacturer's instructions. Alternatively, CD34$^+$ cells were purified from BM or PB leukapheresis product using a PE-conjugated CD34 antibody (clone 563; BD Biosciences — Pharmingen) on a Miltenyi CliniMacs Column (Miltenyi). The number of CD34$^+$ cells isolated represented approximately

1% of the mononuclear cells derived from the nonhuman primate BM or PB after mobilization. Purities of 90%–98% $CD34^+$ cells were obtained.

Vector construction. For GFP-MGMT* SIV vectors (Figure 1A), the open reading frame of the fusion protein GFP-MGMT* was used to replace the GFP cDNA sequence in the parental SIVmac1A11 vector plasmid pCL20cSLFR MSCV-GFP constructed by Hanawa et al. (57) using EcoRI and NotI restriction enzymes. Construction of the fusion protein was described previously (58).

For MGMT*-GFP SIV vectors (Figure 1B), P2A was used to generate a multicistronic expression cassette inserted in the pCL20cSLFR MSCV-GFP backbone. In contrast to multicistronic vectors using internal ribosome entry sites, where multiple proteins are often not expressed at the same level, multicistronic retroviral vectors using 2A peptides to link 2 or several genes have previously been shown to result in stoichiometric production of each protein (59). MGMT* and GFP were amplified and P2A tagged from their cDNAs using primer pairs M5 (5′-TCTCTAGGCGCCGGAATTCCGGATGGACAAGGATTGTGAAATGAAACGCACCACACTGGACAGCCCTTTGGGGAAGCTGGAG-3′), M3 (5′-GGGACCGGGGTTTTCTTCCACGTCTCCTGCTTGCTTTAACAGAGAGAAGTTCGTGGCTCCGGAGTTTCGGCCAGCAGGCGGGGAGCCCGA-3′), G5 (5′-TCCGGAGAGGGCAGAGGAAGTCTGCTAACATGCGGTGACGTCGAGGAGAATCCTGGCCCAATGGTGAGCAAGGGCGAGGAGCTGTTC-3′), and G3 (5′-CCATCGATGGTTACTTGTACAGCTCGTCCATGCCGAGAGTGATCCCGGCGGCGGTCACGAACTCC-3′). A secondary PCR reaction was performed using MGMT*-P2A and P2A-GFP as templates and M5 and G3 as primers. MGMT*-YFP SIV vectors (Figure 1C) were constructed using a similar strategy with primer pairs M5, M3, Y5 (5′-TCCGGAGCCACGAACTTCTCTCTGTTAAAGCAAGCAGGAGACGTGGAAGAAAACCCCGGTCCCATGGTGAGCAAGGGCGAGGAGCTGTTC-3′), and Y3 (5′-CCATCGATGGTTACTTGTACAGCTCGTCCATGCCGAGAGTGATCCCGGCGGCGGTCACGAACTCC-3′).

For MGMT*-HOXB4-GFP SIV vectors (Figure 1D), T2A was used to generate a multicistronic expression cassette inserted in the pCL20cSLFR MSCV-GFP backbone. MGMT*, HOXB4, and GFP were amplified and 2A tagged from their respective cDNAs using primer pairs M5, M3, H5 (5′-TCCGGAGCCACGAACTTCTCTCTGTTAAAGCAAGCAGGAGACGTGGAAGAAAACCCCGGTCCCATGGCTATGAGTTCTTTTTTGATCAACTCA-3′), H3 (5′-TGGGCCAGGATTCTCCTCGACGTCACCGCATGTTAGCAGACTTCCTCTGCCCTCTCCGGAGAGCGCGCGGGGGCCTCCATT-3′), G5, and G3. A secondary PCR reaction was performed using MGMT*-P2A and P2A-HOXB4 as templates and M5 and H3 as primers to generate the product MGMT*-P2A-HOXB4-T2A, which was used as the template together with T2A-GFP for the tertiary PCR using primers M5 and G3 to generate the expression cassette. The expression cassettes were then digested with EcoRI and ClaI and subcloned into the pCL20cSLFR MSCV-GFP backbone.

Virus production. Amphotropic-pseudotyped SIV vector particle conditioned medium was produced as described previously (57). Briefly, 1×10^7 293T cells were seeded onto 10-cm dishes and transfected with a total of 44 μg DNA per dish containing the following plasmids: 12 μg pCAG-SIV gprre; 4 μg pCAG4-RTR-SIV; 4 μg pCAG-Ampho; and 24 μg pCL20cSLFR GFP-MGMT*, MGMT*-YFP, MGMT*-GFP, or MGMT*-HOXB4-GFP. The cells were washed with PBS 18 hours later and cultured in fresh medium for an additional 24 hours. Conditioned medium was then harvested, filtered through a 22-μm nylon filter (Millipore) to remove cellular debris before transduction, concentrated by ultracentrifugation (9,000 *g* for 3 hours), resuspended in X-vivo medium (BioWhittaker Inc.), and frozen at –80°C. Each vector preparation was tested for replication-competent lentivirus as described previously (57). In brief, 5×10^4 HeLa cells were transduced with an equal amount of SIV particles and grown for 2–3 weeks. Conditioned medium was then tested for the presence of SIV p27 using an ELISA kit (Coulter).

Transduction of rhesus repopulating HSCs. For animals RQ4876 and RQ4795, $CD34^+$ cells were cultured at a starting concentration of 1×10^6 cells/ml in filtered vector supernatant (MOI of 1) supplemented with 100 ng/ml recombinant human SCF (rhuSCF; Amgen), 100 ng/ml recombinant human FMS-like tyrosine kinase-3 ligand (rhuFlt-3L; Immunex), 100 ng/ml thrombopoietin (TPO; R&D Systems), and 4 μg/ml protamine sulfate (Sigma-Aldrich) in 6-well plates previously coated with the CH-296 fragment of fibronectin (Retronectin; TaKaRa) per the manufacturers' instructions. Every 24 hours, nonadherent cells were collected, spun down, resuspended in fresh vector supernatant and cytokines, and added back to the same fibronectin-coated plates. At the end of the 96-hour incubation period, transduced cells were removed from the plates using cell scrapers.

For animals RQ4513, RQ4099, and RQ4152, $CD34^+$ cells were prestimulated at 37°C in DMEM supplemented with 10% FCS (HyClone) and 100 ng/ml each of SCF, rhuFlt-3L, and TPO for 24 hours and then transduced on Retronectin-coated plates with vector-containing medium (MOI of 1) for 48 hours, with fresh medium containing cytokines and vector particles provided at the midpoint.

Cells were infused back into each animal conditioned with 2 doses of 450–500 cGy total body irradiation. After 24 hours, 5 μg/kg G-CSF was initiated i.v. daily until the total wbc count reached 6,000 cells/μl. Standard supportive care was administered, including blood product transfusions, fluid and electrolyte management, and antibiotics as needed. Hematopoietic recovery was monitored by daily complete blood counts.

Drug treatment. All drugs were freshly prepared on the day of drug treatment. BG (50 mg; Sigma-Aldrich) was dissolved in 10 ml polyethylene glycol (Fisher Scientific) and further diluted to 2.5 mg/ml with prewarmed (37°C) saline. BCNU (Bristol-Myers Squibb Co.) was diluted according to the manufacturer's instructions and was further diluted in normal saline to a total volume of 18 ml before infusion. TMZ capsules (Schering-Plough) were opened, their content was weighed, and capsules were diluted in sterile H_2O.

For drug treatment to evaluate in vitro hematopoietic chemoprotection, transduced $CD34^+$ cells were exposed in vitro for 1 hour to BG (0–10 μM) followed by exposure to various concentrations of TMZ (0–200 μM) or BCNU (0–10 μM) for an additional 2 hours. Cells were then washed and cultured for an additional 10 days.

For in vivo drug treatment, animals were anesthetized, and Kytril (Roche) was administered prophylactically before drug administration. BG was infused i.v. into the animal at a dose of 120 mg/m^2 over 20 minutes. TMZ was administered at a concentration of 245 mg/m^2 for animals RQ4876 and RQ4795 and in 7 escalating doses for animals RQ4513, RQ4099 and RQ4152 (170, 202, 230, 284, 325, 365, and 450 mg/m^2) via nasogastric tube or by direct oral administration of capsules over 5 minutes 1 hour after the end of BG infusion. Treatment was repeated daily for 5 consecutive days. BCNU was administered i.v. over a 5-minute period at a dose of 20 mg/m^2 30 minutes after the end of BG infusion. A repeat dose of BG was administered i.v. at a concentration of 120 mg/m^2 approximately 7 hours after the end of the first BG infusion.

Analysis of transduction efficiency. For RQ4876 and RQ4795, we used SIV vectors expressing GFP-MGMT* fusion protein, and transduction efficiency was determined by flow cytometry analysis using a Coulter FC500 analyzer (Beckman Coulter).

For RQ4513 and RQ4099, MGMT*-YFP versus MGMT*-HOXB4-GFP vectors were used, allowing for GFP versus YFP identification of cells in the competitive repopulating study. Flow cytometric analysis was performed for GFP and YFP expression using a FACSVantage SE instrument with FACSDiva software (version 5.0; BD). To quantitate GFP^+ and YFP^+ cells in immunophenotypically defined subsets of PB cells, the following PE-con-

jugated antibodies were used: CD11b (clone ICRF44), CD14 (clone MSE2), CD16 (clone 3G8), CD3 (clone SP34-2), CD4 (clone MT310), CD8 (clone DK25), and CD20 (clone 2H7; all from BD Biosciences — Pharmingen).

For RQ4152, both vectors used GFP as expression marker. Therefore, Southern blot analysis was used to distinguish the 2 subsets of cells. Purified PB DNA was digested with BsrGI, which liberated a 2.3-kb fragment for the MGMT*-HOXB4-GFP vector and a 1.5-kb fragment for the MGMT*-GFP vector, and hybridized with a probe corresponding to a partial MGMT* sequence.

Evaluation of vector ISs. Purified PB DNA was prepared at different time points after transplant using Puregene DNA extraction kit (Gentra Systems), and LAM-PCR was performed as described previously (57). Briefly, 100 ng DNA was amplified using a SIV-LTR–specific 5′-biotinylated primer and digested with ApoI enzyme and then ligated to a linker cassette. Nested PCR was performed using SIV-LTR–specific and linker-specific primers. Next, 5 μl of the PCR products were separated on a high-resolution spreadex gel (Elchrom Scientific), and each band was then picked from the gel using a bandpick (Elchrom Scientific) and amplified using the nested PCR primer pair and sequenced directly. We considered a sequence as a genuine retroviral IS only if it (a) juxtaposed to the vector LTR, (b) yielded a unique best hit by BLAT software (http://genome.ucsc.edu/cgi-bin/hgBlat), and (c) showed at least 90% identity to the July 2003 human genome assembly (60, 61). Annotations for CAGs were determined using the Sanger Institute Human Cancer Gene Census Database (http://www.sanger.ac.uk/genetics/CGP/Census) (62).

Demonstration of common vector ISs. Using DNA isolated from the BM of rhesus macaque RQ4876 more than 1 year after transplant, we performed LAM-PCR and isolated 10 ISs. Demonstration of common lentiviral ISs in sorted subpopulations of the PB (T cells, B cells, and granulocytes) collected before in vivo selection (2 months after transplant), after BG/TMZ selection (12 months), and after BG/BCNU treatment (31 months) was performed by PCR using 1 vector LTR primer (5′-AGAGCGACTGACTACATAGC-3′) and 1 genomic primer spanning a region of each IS (IS 1, 5′-TTAGATGTGCTGGGGTGGCATAAGAAGC-3′; IS 2, 5′-AATTCTGCAGATATCCAGCACAGTGG-3′). Each DNA sample was amplified using β-actin–specific primers as positive control (forward, 5′-AAGAGAGGCATCCTCACCCT-3′; reverse, 5′-GAAGGTGTGGTGCCAGATTTTC-3′).

MGMT activity assay. Transduced or naive rhesus macaque BM cells were sonicated (30 seconds ×2 in 50 mM Tris-HCl, pH 7.6; 5 mM DTT; and 0.1 mM EDTA; XL-series sonicator; Misonix Inc.) and centrifuged to collect supernatant. MGMT activity was assayed by incubation of supernatants for 30 minutes at 37°C with [^{3}H]-methylated DNA substrate in the presence or absence of 200 μM BG, followed by acid hydrolysis and separation of free bases on HPLC; activity was expressed as O^6-methylguanine transferred to MGMT (fmol/mg protein; Bradford protein assay; ref. 63).

Statistics. Data were analyzed using the unpaired Student's *t* test using Sigma Plot software. All statistical tests were 2 sided. A *P* value of 0.05 was considered to be statistically significant.

Acknowledgments

We thank Arthur Nienhuis for scientific discussion. This work was supported in part by the intramural research program of NHLBI and NIAID, NIH; by NHLBI grant P01 HL 53749; by Cancer Center Support Grant P30 CA 21765; by the Assisi Foundation of Memphis; and by the American Lebanese Syrian Associated Charities.

Received for publication September 19, 2008, and accepted in revised form April 15, 2009.

Address correspondence to: Andre Larochelle, National Heart, Lung and Blood Institute, National Institutes of Health, 9000 Rockville Pike, Building 10CRC, Room 3E-5256, Bethesda, Maryland 20892, USA. Phone: (301) 451-7139; Fax: (301) 496-8396; E-mail: larochea@nhlbi.nih.gov.

1. Nienhuis, A.W., Dunbar, C.E., and Sorrentino, B.P. 2006. Genotoxicity of retroviral integration in hematopoietic cells. *Mol. Ther.* **13**:1031–1049.
2. Nienhuis, A.W. 2008. Development of gene therapy for blood disorders. *Blood.* **111**:4431–4444.
3. Ferguson, C., Larochelle, A., and Dunbar, C.E. 2005. Hematopoietic stem cell gene therapy: dead or alive? *Trends Biotechnol.* **23**:589–597.
4. Horn, P.A., Morris, J.C., Neff, T., and Kiem, H.P. 2004. Stem cell gene transfer--efficacy and safety in large animal studies. *Mol. Ther.* **10**:417–431.
5. Cavazzana-Calvo, M., et al. 2000. Gene therapy of human severe combined immunodeficiency (SCID)-X1 disease. *Science.* **288**:669–672.
6. Neff, T., Beard, B.C., and Kiem, H.P. 2006. Survival of the fittest: in vivo selection and stem cell gene therapy. *Blood.* **107**:1751–1760.
7. Podda, S., et al. 1992. Transfer and expression of the human multiple drug resistance gene into live mice. *Proc. Natl. Acad. Sci. U. S. A.* **89**:9676–9680.
8. Sorrentino, B.P., et al. 1992. Selection of drug resistant bone marrow cells in vivo after retroviral transfer of human MDR1. *Science.* **257**:99–103.
9. Allay, J.A., et al. 1998. In vivo selection of retrovirally transduced hematopoietic stem cells. *Nat. Med.* **4**:1136–1143.
10. Davis, B.M., Koc, O.N., and Gerson, S.L. 2000. Limiting numbers of G156A O(6)-methylguanine-DNA methyltransferase- transduced marrow progenitors repopulate nonmyeloablated mice after drug selection. *Blood.* **95**:3078–3084.
11. Ragg, S., et al. 2000. Direct reversal of DNA damage by mutant methyltransferase protein protects mice against dose-intensified chemotherapy and leads to in vivo selection of hematopoietic stem cells. *Cancer Res.* **60**:5187–5195.
12. Sawai, N., et al. 2001. Protection and in vivo selection of hematopoietic stem cells using temozolomide, O(6)-benzylguanine, and an alkyltransferase-expressing retroviral vector. *Mol. Ther.* **3**:78–87.
13. Persons, D.A., et al. 2004. Transient in vivo selection of transduced peripheral blood cells using antifolate drug selection in rhesus macaques that received transplants with hematopoietic stem cells expressing dihydrofolate reductase vectors. *Blood.* **103**:796–803.
14. Hibino, H., et al. 1999. The common marmoset as a target preclinical primate model for cytokine and gene therapy studies. *Blood.* **93**:2839–2848.
15. Licht, T., et al. 2002. Drug selection with paclitaxel restores expression of linked IL-2 receptor gamma -chain and multidrug resistance (MDR1) transgenes in canine bone marrow. *Proc. Natl. Acad. Sci. U. S. A.* **99**:3123–3128.
16. Crone, T.M., Kanugula, S., and Pegg, A.E. 1995. Mutations in the Ada O6-alkylguanine-DNA alkyltransferase conferring sensitivity to inactivation by O6-benzylguanine and 2,4-diamino-6-benzyloxy-5-nitrosopyrimidine. *Carcinogenesis.* **16**:1687–1692.
17. Loktionova, N.A., Xu-Welliver, M., Crone, T.M., Kanugula, S., and Pegg, A.E. 1999. Protection of CHO cells by mutant forms of O6-alkylguanine-DNA alkyltransferase from killing by 1,3-bis-(2-chloroethyl)-1-nitrosourea (BCNU) plus O6-benzylguanine or O6-benzyl-8-oxoguanine. *Biochem. Pharmacol.* **58**:237–244.
18. Gerull, S., Beard, B.C., Peterson, L.J., Neff, T., and Kiem, H.P. 2007. In vivo selection and chemoprotection after drug resistance gene therapy in a nonmyeloablative allogeneic transplantation setting in dogs. *Hum. Gene Ther.* **18**:451–456.
19. Neff, T., et al. 2003. Methylguanine methyltransferase-mediated in vivo selection and chemoprotection of allogeneic stem cells in a large-animal model. *J. Clin. Invest.* **112**:1581–1588.
20. Neff, T., et al. 2005. Polyclonal chemoprotection against temozolomide in a large-animal model of drug resistance gene therapy. *Blood.* **105**:997–1002.
21. Pollok, K.E., et al. 2003. In vivo selection of human hematopoietic cells in a xenograft model using combined pharmacologic and genetic manipulations. *Hum. Gene Ther.* **14**:1703–1714.
22. Zielske, S.P., Reese, J.S., Lingas, K.T., Donze, J.R., and Gerson, S.L. 2003. In vivo selection of MGMT(P140K) lentivirus-transduced human NOD/SCID repopulating cells without pretransplant irradiation conditioning. *J. Clin. Invest.* **112**:1561–1570.
23. Stupp, R., et al. 2005. Radiotherapy plus concomitant and adjuvant temozolomide for glioblastoma. *N. Engl. J. Med.* **352**:987–996.
24. Perkins, A.C., and Cory, S. 1993. Conditional immortalization of mouse myelomonocytic, megakaryocytic and mast cell progenitors by the Hox-2.4 homeobox gene. *EMBO J.* **12**:3835–3846.
25. Sauvageau, G., et al. 1995. Overexpression of HOXB4 in hematopoietic cells causes the selective expansion of more primitive populations in vitro and in vivo. *Genes Dev.* **9**:1753–1765.
26. Antonchuk, J., Sauvageau, G., and Humphries, R.K. 2002. HOXB4-induced expansion of adult hematopoietic stem cells ex vivo. *Cell.* **109**:39–45.
27. Zhang, X.B., et al. 2006. Differential effects of HOXB4 on nonhuman primate short- and long-term repopulating cells. *PLoS Med.* **3**:e173.
28. Sawai, N., Persons, D.A., Zhou, S., Lu, T., and Sorrentino, B.P. 2003. Reduction in hematopoietic stem cell numbers with in vivo drug selection can

be partially abrogated by HOXB4 gene expression. *Mol. Ther.* **8**:376–384.
29. Panetta, J.C., et al. 2003. Population pharmacokinetics of temozolomide and metabolites in infants and children with primary central nervous system tumors. *Cancer Chemother. Pharmacol.* **52**:435–441.
30. Quinn, J.A., et al. 2005. Phase I trial of temozolomide plus O6-benzylguanine for patients with recurrent or progressive malignant glioma. *J. Clin. Oncol.* **23**:7178–7187.
31. Hematti, P., et al. 2004. Distinct genomic integration of MLV and SIV vectors in primate hematopoietic stem and progenitor cells. *PLoS Biol.* **2**:e423.
32. Mitchell, R.S., et al. 2004. Retroviral DNA integration: ASLV, HIV, and MLV show distinct target site preferences. *PLoS Biol.* **2**:E234.
33. Bushman, F., et al. 2005. Genome-wide analysis of retroviral DNA integration. *Nat. Rev. Microbiol.* **3**:848–858.
34. Kim, Y.J., et al. 2009. Sustained high level polyclonal hematopoietic marking and transgene expression four years following autologous transplantation of rhesus macaques with SIV lentiviral vector transduced CD34+ cells. *Blood*. Online publication ahead of print. doi:10.1182/blood-2008-10-185199.
35. Milsom, M.D., et al. 2008. Reciprocal relationship between O6-methylguanine-DNA methyltransferase P140K expression level and chemoprotection of hematopoietic stem cells. *Cancer Res.* **68**:6171–6180.
36. Hanawa, H., et al. 2004. Extended beta-globin locus control region elements promote consistent therapeutic expression of a gamma-globin lentiviral vector in murine beta-thalassemia. *Blood.* **104**:2281–2290.
37. Hanawa, H., Persons, D.A., and Nienhuis, A.W. 2002. High-level erythroid lineage-directed gene expression using globin gene regulatory elements after lentiviral vector-mediated gene transfer into primitive human and murine hematopoietic cells. *Hum. Gene Ther.* **13**:2007–2016.
38. Persons, D.A., et al. 2003. Successful treatment of murine beta-thalassemia using in vivo selection of genetically modified, drug-resistant hematopoietic stem cells. *Blood.* **102**:506–513.
39. Hong, S., et al. 2007. Functional analysis of various promoters in lentiviral vectors at different stages of in vitro differentiation of mouse embryonic stem cells. *Mol. Ther.* **15**:1630–1639.
40. Wang, L., Haas, D., Halene, S., and Kohn, D. 2003. Effects of the negative control region on expression from retroviral LTR. *Mol. Ther.* **7**:438–439.
41. Challita, P.M., et al. 1995. Multiple modifications in cis elements of the long terminal repeat of retroviral vectors lead to increased expression and decreased DNA methylation in embryonic carcinoma cells. *J. Virol.* **69**:748–755.
42. Robbins, P.B., et al. 1997. Increased probability of expression from modified retroviral vectors in embryonal stem cells and embryonal carcinoma cells. *J. Virol.* **71**:9466–9474.
43. Halene, S., et al. 1999. Improved expression in hematopoietic and lymphoid cells in mice after transplantation of bone marrow transduced with a modified retroviral vector. *Blood.* **94**:3349–3357.
44. Lois, C., Hong, E.J., Pease, S., Brown, E.J., and Baltimore, D. 2002. Germline transmission and tissue-specific expression of transgenes delivered by lentiviral vectors. *Science.* **295**:868–872.
45. Shepherd, B.E., et al. 2007. Hematopoietic stem-cell behavior in nonhuman primates. *Blood.* **110**:1806–1813.
46. Abkowitz, J.L., Golinelli, D., Harrison, D.E., and Guttorp, P. 2000. In vivo kinetics of murine hemopoietic stem cells. *Blood.* **96**:3399–3405.
47. Zhou, S., et al. 2001. The ABC transporter Bcrp1/ABCG2 is expressed in a wide variety of stem cells and is a molecular determinant of the side-population phenotype. *Nat. Med.* **7**:1028–1034.
48. Bunting, K.D. 2002. ABC transporters as phenotypic markers and functional regulators of stem cells. *Stem Cells.* **20**:11–20.
49. Moreb, J.S. 2008. Aldehyde dehydrogenase as a marker for stem cells. *Curr. Stem Cell Res. Ther.* **3**:237–246.
50. Hess, D.A., et al. 2004. Functional characterization of highly purified human hematopoietic repopulating cells isolated according to aldehyde dehydrogenase activity. *Blood.* **104**:1648–1655.
51. Sung, L.Y., et al. 2006. Differentiated cells are more efficient than adult stem cells for cloning by somatic cell nuclear transfer. *Nat. Genet.* **38**:1323–1328.
52. Thorsteinsdottir, U., et al. 1997. Overexpression of HOXA10 in murine hematopoietic cells perturbs both myeloid and lymphoid differentiation and leads to acute myeloid leukemia. *Mol. Cell Biol.* **17**:495–505.
53. Zhang, X.B., et al. 2008. High incidence of leukemia in large animals after stem cell gene therapy with a HOXB4-expressing retroviral vector. *J. Clin. Invest.* **118**:1502–1510.
54. Larochelle, A., et al. 2006. AMD3100 mobilizes hematopoietic stem cells with long-term repopulating capacity in nonhuman primates. *Blood.* **107**:3772–3778.
55. Donahue, R.E., et al. 1996. Peripheral blood CD34+ cells differ from bone marrow CD34+ cells in Thy-1 expression and cell cycle status in nonhuman primates mobilized or non mobilized with granulocyte colony-stimulating factor and/or stem cell factor. *Blood.* **87**:1644–1653.
56. Dunbar, C.E., et al. 1996. Improved retroviral gene transfer into murine and rhesus peripheral blood or bone marrow repopulating cells primed in vivo with stem cell factor and granulocyte colony-stimulating factor. *Proc. Natl. Acad. Sci. U. S. A.* **93**:11871–11876.
57. Hanawa, H., et al. 2004. Efficient gene transfer into rhesus repopulating hematopoietic stem cells using a simian immunodeficiency virus-based lentiviral vector system. *Blood.* **103**:4062–4069.
58. Choi, U., et al. 2004. Nuclear-localizing O6-benzylguanine-resistant GFP-MGMT fusion protein as a novel in vivo selection marker. *Exp. Hematol.* **32**:709–719.
59. Szymczak, A.L., et al. 2004. Correction of multigene deficiency in vivo using a single 'self-cleaving' 2A peptide-based retroviral vector. *Nat. Biotechnol.* **22**:589–594.
60. Karolchik, D., et al. 2007. Comparative genomic analysis using the UCSC genome browser. *Methods Mol. Biol.* **395**:17–34.
61. Kent, W.J. 2002. BLAT — the BLAST-like alignment tool. *Genome Res.* **12**:656–664.
62. Futreal, P.A., et al. 2004. A census of human cancer genes. *Nat. Rev. Cancer.* **4**:177–183.
63. Bradford, M.M. 1976. A rapid and sensitive method for the quantitation of microgram quantities of protein utilizing the principle of protein-dye binding. *Anal. Biochem.* **72**:248–254.